Vortex-Front Propagation in Rayleigh-Bénard Convection

Jay Fineberg and Victor Steinberg
Department of Nuclear Physics, Weizmann Institute of Science, Rehovot 76100, Israel
(Received 8 December 1986)

We present experimental measurements of the velocity of a convective vortex front propagating into an unstable conductive state in a Rayleigh-Bénard system for the wide range of ε ($\varepsilon \equiv \Delta T/\Delta T_c - 1$) between 4×10^{-4} and 2.5×10^{-1}. The results are found to be in excellent quantitative agreement with the theoretical predictions following from an amplitude equation, exhibiting a sharp selection mechanism in the propagation velocity. Wave-number selection by this dynamical mechanism is also studied.

PACS numbers: 47.25.−c

Much effort has been devoted over the last several years to an understanding of the existence of pattern and wave-number selection in various nonequilibrium systems. It was recently suggested that a particular dynamical mechanism[1] leads to the selection of a specific state for a large class of pattern-forming systems. This mechanism, coined "pattern propagation,"[1] demonstrates both pattern selection and the sharp selection of the velocity of the boundary between stable and unstable states. This process can be initiated by a local perturbation of the stationary but unstable uniform state. The perturbation will grow locally into a pattern, and this pattern will spread out into the unstable state. The front which separates the stable and unstable states will propagate with a well-defined velocity. Moreover, it is predicted[1] that a unique wave number will be selected behind the front for a fully developed pattern. This selection mechanism, which is an intrinsic property of the system, independent of details of initial conditions and external perturbations, results in a unique final state.

This phenomenon has been discussed for simple theoretical models,[1,2] some of which are expected to be an exact description of real systems, like Rayleigh-Bénard (R-B) convection, in the limit of $\varepsilon \to 0$ and for spatial variations on a scale larger than a wavelength. For small ε these models (and equations of motion of real systems) can be approximated by a Ginsburg-Landau-type equation,[3]

$$\tau_0 \partial_t A = \varepsilon A + \xi_0^2 \partial_x^2 A - g|A|^2 A, \tag{1}$$

where A is a complex, slowly varying amplitude of the periodic state. Full spatial and temporal variation of the physical variables is given by a stream function of the form $\psi = \mathrm{Re}[A\exp(iq_0 x)]$. The scales ξ_0 and τ_0 follow from linear stability analysis. A striking fact is that Eq. (1) results in a pattern-front propagation which occurs at the unique velocity[1,2,4]

$$V = \tilde{V}\xi_0 \varepsilon^{1/2}\tau_o^{-1}, \tag{2}$$

where $\tilde{V} = 2$. Since this selection principle is a general property of Eq. (1),[4] which also precisely coincides with the marginal-stability hypothesis for Eq. (1),[1] one expects that the prediction (2) would apply to real systems. The only experiment on propagating fronts to date has been done on Taylor-vortex flow,[5] and has demonstrated the existence of a unique velocity of vortex-front propagation and wave-number selection under dynamic conditions. However, an important problem, that the observed front-propagation velocity was about half the predicted value and lies in a linearly unstable region,[1,2] remains unresolved.

In this Letter we present experimental measurements of the front-propagation velocity and of the wavelength of the rolls formed behind the front in the Rayleigh-Bénard system for the wide range of ε between 4×10^{-4} and 2.5×10^{-1}. The experiment was done on pure water at 30.2 °C (Prandtl number $P = 5.373$). Our experimental apparatus is an improved version of the one described elsewhere.[6] The temperature stability of the bottom plate during many hours and rms noise were better than 0.1 mK. The resolution of the computer-enhanced shadowgraph visualization technique was improved considerably and gave us an opportunity to resolve patterns for $\varepsilon < 10^{-4}$. Simultaneously we were able to reach about the same level of resolution for ε in heat-transport measurements.

A key point of the successful experiment was to work at small enough ε in order to get a reasonable number of rolls behind the front before the occurrence of spontaneous nucleation of the rolls. Since the critical slowing down, which defines the waiting time until spontaneous nucleation, is inversely proportional to ε, and the time of the front propagation is inversely proportional to $\sqrt{\varepsilon}$, it is easy to estimate the value, ε_0, for which the vortex front advances a distance of the order of $(1/m)$th of the cell length, l. One obtains

$$\varepsilon_0 = (\xi_0 \tilde{V} mnd/l)^2, \tag{3}$$

where d is the cell height. The numerical factor, n, was used since the nucleated pattern could be distinguished from noise only after time $\tau = n\tau_0\varepsilon^{-1}$, where from our experiment $n = 3$–4. For our cell with twelve pairs of

rolls Eq. (3) leads to $\varepsilon_0 \simeq 10^{-3}(mn)^2$. Thus we can expect to observe propagating patterns in the full cell ($m=1$) without spontaneous nucleation up to $\varepsilon \lesssim 10^{-2}$ and for a half-full cell ($m=2$) up to $\varepsilon \approx 0.1$.

Another crucial point in the experiment is the special design of the cell which is used to avoid the inducing of long rolls, parallel to the long side of the cell, and the pinning of the rolls by the lateral walls during propagation.[7] Cell dimensions and their cross sections are presented in the inset of Fig. 1. The length of the cell, l, is 75 mm, so that its aspect ratio is about 27.3. In spite of this we observed a stable steady state corresponding to twelve roll pairs which remained stable up to, at least, $\varepsilon \simeq 0.2$.[8] In order to heat from the side, a 0.1-mm resistance wire was glued inside one of the cell's short sides. Thin fins along the long sides of the cell provide almost free boundary conditions. As a result of these boundary conditions the possible induction of long rolls during propagation was avoided, a negligibly small healing length along the rolls was obtained, and smooth motion of the rolls without pinning and bending was observed.

A third point crucial to the experiment's success was to prove experimentally that a local perturbation of the unstable conductive state does not produce patterns in the interior of the cell, and thus does not change the nature of the initial state. By side heating, on the one hand, we produce an imperfection. On the other hand, this imperfection should be small enough in order to be indistinguishable from noise in the range of ε where we performed the experiment. A sensitive test of the degree of imperfection is the "rounding" of the transition to a convective state observed in heat-transport measurement. Figure 1 shows the dependence of the Nusselt number N (i.e., ratio of the effective heat transport through a fluid layer to that due to the thermal conduction alone) versus the temperature difference, ΔT, across the layer without and with side heating ($q_s/q_c = 0.014$, where q_s and q_c are the lateral and critical heat flux, respectively). The rounding due to side heating does not exceed 0.1% (without side heating it is less than 0.03%). It is possible to conclude from both plots in Fig. 1 that side heating does not change the final state beyond the insignificant rounding, which still does not exceed values reached in the best experiments on convection.[9]

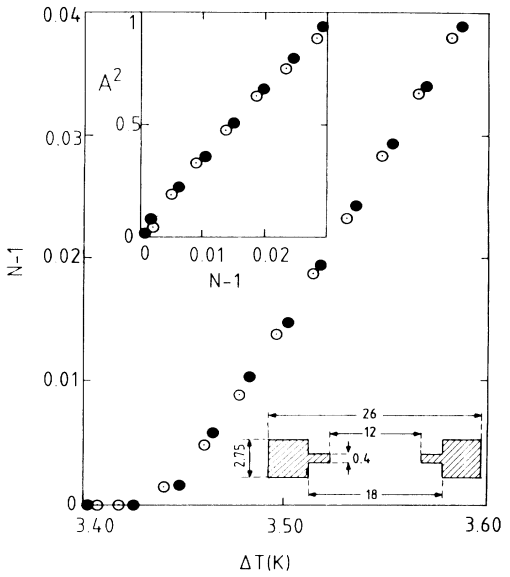

FIG. 1. Convective contribution, $N-1$, to heat transport as a function of the temperature difference across the cell with (open circles) and without (solid circles) side heating. Upper inset: Square of light intensity amplitude vs $N-1$ with and without side heating. Lower inset: Cross section and dimensions of the cell.

Special care was taken to avoid a geometrical imperfection in the cell. This, probably, was the most severe limitation to performing the experiment at small ε. Indeed, naively even a 1-μm variation in the cell height results in an ε variation on the order of 10^{-3}. By using interferometric methods we adjusted the geometrical variation in the height to the level of about 1 μm.

The experiment was performed by our simultaneously increasing the heat flux from an initial state at $\varepsilon_i < 0$ (typical value of $\varepsilon_i = -0.015$) to a supercritical value, and switching on the side heater (typically to a value of $q_s/q_c = 0.014$). Following the sudden increase in heat flux, the temperature difference across the cell jumped from $\varepsilon_i < 0$ to $\varepsilon_1 > 0$ almost instantaneously (much less than our typical sampling time) and the vortex front induced near the side-heated wall started to propagate into the unstable conductive state. The induced vortex pair at the side wall as well as the propagation of the vortex front into the unstable state at $\varepsilon_1 > 0$ are clearly shown in Fig. 2. A contour plot of successive light-intensity profiles across the cell with a time difference between successive lines of about 25 sec is presented (every third

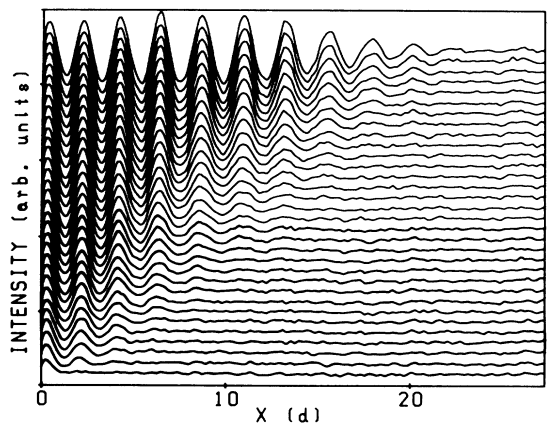

FIG. 2. Contour plot of the light intensity profiles as a function of position along the length of the cell, at time intervals of $0.42t_v$. Time increases upward.

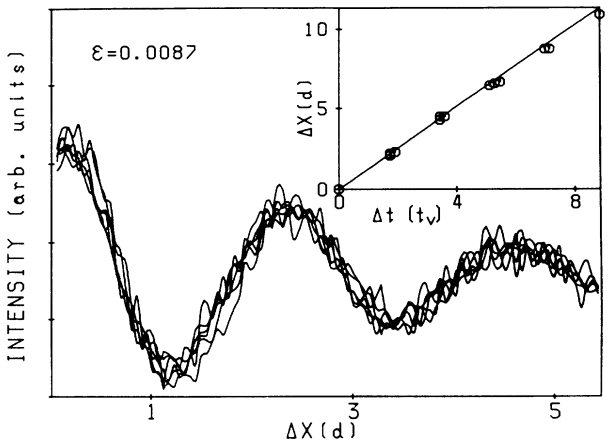

FIG. 3. The superposition of six successive front profiles. Each profile was obtained after the front traveled a distance of λ along the cell. Inset: Relative positions between the six profiles as a function of their time differences. The solid line is the theoretically predicted velocity.

line is shown). Each profile on the contour plot is a result of averaging in space (of 10% of the cell) and in time (of 100 pictures). We measured the vortex-front propagation velocity by fitting the front with itself at various time intervals. Figure 3 shows an example of the superposition of the rolls defining the front taken at six different time intervals. The front's velocity was then determined by our dividing the shift in their position along the cell, Δx, by the corresponding time interval, Δt. The inset in Fig. 3 shows the various values of Δx vs Δt (fifteen in all) determined by the six profiles shown. The data are consistent with the constant velocity predicted from Eq. (2).

The resolution of the method for front-propagation-velocity evaluation is limited by the resolution in the distance measurement and by the resolution of the sampling time, Δt, in the experiment relative to the characteristic time of front propagation. It is easy to show that the latter uncertainty, due to finite sampling frequency, is dominant and is given by $\delta t \simeq \xi_0 \tau_0^{-1} \sqrt{\varepsilon} \Delta t / t_v$, where $t_v = d^2/\kappa$ is the vertical diffusion time, and κ is the thermal diffusivity ($\kappa = 1.43 \times 10^{-3}$ cm^2 sec^{-1}). In our experiment Δt was varied from about 20 sec for small ε to about 4 sec for large ε. We then get an uncertainty in the propagation velocity of up to 15% (we used as estimates[10] $\xi_0^2 = 0.148$ and $\tau_0^{-1} = 6.90$ at $P = 5.373$). This uncertainty was reduced drastically by our fitting many pairs of front profiles in the same run. Typically we had about 100 successive light-intensity profiles in a run before spontaneous nucleation occurred. Theoretically this provided about 1000 data points for velocity evaluation at each ε, but practically it was enough to take up to 70 data points.

Theoretical predictions for the front propagation velocity were confirmed by our data in a wide range of ε between 4×10^{-4} and 2.5×10^{-1}, as shown in Fig. 4.[11] The line drawn through the data is the theoretical prediction. The inset in Fig. 4 shows the same data on a

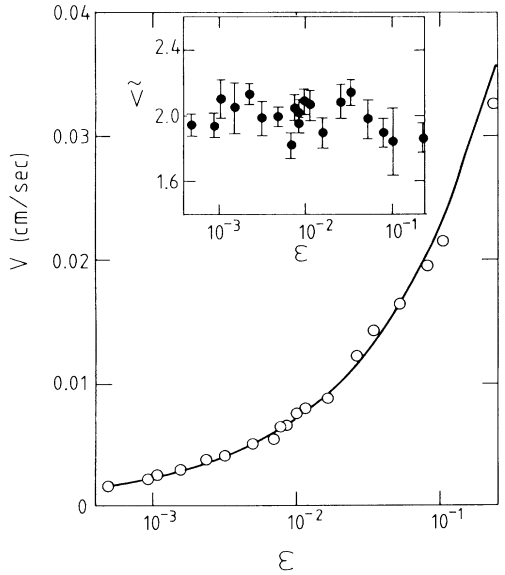

FIG. 4. Vortex-front velocity as a function of ε. The solid line is theoretically predicted by Eq. (2). Inset: The same data presented on a high-resolution plot.

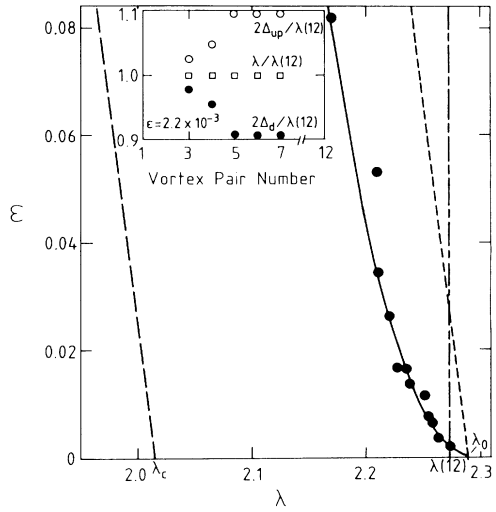

FIG. 5. Selected wavelength as a function of ε. The solid line is the best fit to the data. The dashed line shows the locus of maximum growth rate (Dominguez-Lerma, Ahlers, and Cannel, Ref. 14) (the second dashed line is shifted to λ_0). the dash-dotted line corresponds to the steady-state value of λ with twelve roll pairs. Inset: Structure of the periodic state behind the front.

high-resolution plot. From both representations it is clear that the last two points at higher ε already show a slight deviation from the rest of the data. The average value for $\tilde{V}$ is $\tilde{V}=2.01$ with a standard deviation of 0.02.[12]

Finally we address the problem of the selection of the wavelength, λ of the rolls by the front propagation mechanism. To determine λ we neglected the first two or three roll pairs near the wall and measured the widths of upflow, Δ_{up}, and downflow, Δ_d, regions which correspond to the distances between successive nodes in the light-intensity profiles. The inset in Fig. 5 shows the results of the measurements for one particular run. It is clearly seen that Δ_{up} is (by mass conservation) larger than Δ_d although the local wavelength is practically constant. This effect lessens as we approach steady state. A similar effect, where, in contrast, $\Delta_{up}-\Delta_d$ increased away from the front, was observed in a numerical calculation of the Navier-Stokes equations for Taylor-vortex flow.[13] Such a complicated spatial-pattern evolution behind the propagating front lies beyond the scope of the amplitude equation (1). Results of our measurements of the averaged local wavelength of the vortices behind the front as a function of ε are presented in Fig. 5.

At the smallest ε the wavelength, λ^*, selected by the front is close to that obtained in a steady state.[8] As ε increases, λ^* decreases. We can fit our data within experimental error by a function $\lambda^*/\lambda_0=1-b\sqrt{\varepsilon}$, where $\lambda_0=2.29$ and $b=0.18$. This dependence is surprisingly close to that obtained from marginal-stability analysis and numerical studies of the Swift-Hohenberg model,[1,2] i.e., $\lambda^*/\lambda_c=1-0.16\sqrt{\varepsilon}$.

This work was supported in part by the U.S.- Israel Binational Scientific Foundation Grant No. 8400256, and the Minerva Foundation. One of us (V.S.) acknowledges the support of the M. M. Boukstein Career Development Fund.

[1]G. Dee and J. S. Langer, Phys. Rev. Lett. **50**, 383 (1985).

[2]E. Ben-Jacob, H. Brand, G. Dee, L. Kramer, and J. S. Langer, Physica (Amsterdam) **14D**, 348 (1985).

[3]A. C. Newell and J. A. Whitehead, J. Fluid Mech. **38**, 279 (1969); L. A. Segel, J. Fluid Mech. **38**, 203 (1969).

[4]A. Kolmogorov, I. Petrovsky, and N. Pisconov, Bull. Univ. Moscow Ser. Internat. Sec. A **1**, 1 (1937); D. G. Aronson and H. F. Weinberger, in *Partial Differential Equations and Related Topics,* edited by J. A. Goldstein, Lecture Notes in Mathematics, Vol. 466 (Springer, New York, 1975), p. 5.

[5]G. Ahlers and D. S. Cannell, Phys. Rev. Lett. **50**, 1583 (1983).

[6]E. Moses and V. Steinberg, Phys. Rev. A **34**, 693 (1986).

[7]We are grateful to G. Ahlers who suggested the use of this design; also C. W. Meyer, G. Ahlers, and D. S. Cannell, Bull. Am. Phys. Soc. **31**, 473 (1986).

[8]It was possible to obtain thirteen roll pairs by "quenching." These were stable in some range of ε. However, for $\varepsilon<6\times10^{-3}$ this state became unstable relative to the state with twelve roll pairs. Thus, $\lambda_{eq}=\lambda(12)=2.27d$ was very different from $\lambda_c=2.016d$. We believe that this is due to the special cell design; we do not have another reasonable explanation.

[9]V. Steinberg, G. Ahlers, and D. S. Cannell, Phys. Scr. **32**, 534 (1985).

[10]M. C. Cross, Phys. Fluids **23**, 1727 (1980).

[11]The value of ε for each run was obtained in two ways: first, by deducing it from the independent N vs ΔT measurements presented in Fig. 1, and second, by obtaining ε from the light-intensity amplitude of the roll structure at the steady state, which was a final state for each run. In order to compare these two methods we plot a square of the amplitude averaged over the sixth to eighth rolls vs N (inset in Fig. 1). The straight line which passes through the origin represents the data reasonably well within the error bars.

[12]We found no influence on the front propagation velocity resulting from the rate of side heating for values of q_s/q_c between 0.003 and 0.036.

[13]M. Lücke, M. Mihelcic, and K. Wingerath, Phys. Rev. Lett. **52**, 625 (1984), and Phys. Rev. A **31**, 396 (1985).

[14]M. A. Dominguez-Lerma, G. Ahlers, and D. S. Cannell, Phys. Fluids **27**, 856 (1984).